

Supplementary material

- 1. Detailed methods**
 - a. Immunohistochemistry
 - b. Table 1s. List of antibodies used and their specificities
 - c. RNA in situ hybridization and immunohistochemical analysis
 - d. SARS-CoV2 RNA PCR evaluation
 - e. Double immunofluorescence for the identification of NETs
 - f. Negative staining electron microscopy
 - g. Transmission Electron Microscopy
- 2. Table 2s. Main clinical data of COVID-19 positive patients and their newborns**
- 3. Table 3s. Main clinical data of COVID-19 negative patients and their newborns**
- 4. Table 4s. Main morphological changes observed in the 86 non COVID-19 placentas**
- 5. Supplementary figures**
- 6. References**

Detailed methods

Immunohistochemistry

Formalin-fixed paraffin embedded (FFPE) tissue sections were used for immunohistochemical staining. For SARS-CoV2 proteins a manual procedure was used: upon microwave oven epitope retrieval in TRIS-EDTA buffer (pH 9.00) with 2+3 cycles (5 minutes each) at 1000W and 750W respectively, sections were incubated at room temperature with primary antibodies for two hours, followed by incubation with EnVision+System-HRP Labelled Polymer Anti-Rabbit (Dako) for 30 minutes. Chromogenic reaction was done using Diaminobenzidine. The slides were finally counterstained with Meyer's Haematoxylin.

For double immunohistochemistry, after completing the first immune reaction (see above), the second reaction was visualized using Mach 4 MR-AP (Biocare Medical, Concord, CA, USA), followed by Ferangi Blue (Biocare Medical) as chromogen¹.

Table 1s. List of antibodies used and their specificities.

Antibodies (Clone; Source *)	Antigen retrieval (cycles)**	Antibody dilution	Double stain combinations	Source
SARS-CoV-2 (2019-nCoV) Spike Antibody (007; mR)	MwTE(5c)	1:100	(A)(B)(C)(D)	Sino Biological (Beijing, CHN)
SARS-CoV-2 (2019-nCoV) Nucleocapsid Antibody (pR)	MwTE(5c)	1:2500		Sino Biological
ARGINASE-1 (SP156; mM)	MwE(5c)	1:100		Cell Marque (St.Louis, MI, U.S.)
C4d (SP91; mM)	MwE(5c)	Ready to use		Cell Marque
CD3 (LN10; mM)	MwE(3c)	1:100		Leica Biosystem (Wetzlar, D)
CD4 (4B12; mM)	MwE(5c)	1:50		Thermo Scientific (Waltham, MA, U.S.)
CD8 (C8/144B; mM)	MwE(3c)	1:50		Agilent (Santa Clara, CA, U.S.)
CD10 (56C6; mM)	MwE(5c)	1:50	(E)	Leica Biosystem
CD14 (7; mM)	MwE(5c)	1:50	(A)(F)(G)	Leica Biosystem
CD15 (MMA; mM)	MwE(5c)	1:250		Thermo Scientific
CD16 (SP175; mM)	MwE(5c)	Ready to use		Cell Marque
CD20 (L26; mM)	MwE(3c)	1:250		Leica Biosystem (Nussloch, D)
CD34 (QBEND/10; mM)	MwE(3c)	1:200	(C)(H)(I)(J)	Leica Biosystem
CD38 (SPC32; mM)	MwE(3c)	1:200		Leica Biosystem
CD56 (123C3.D5; mM)	MwE(5c)	1:50		Emergo Europe (Prinsessegracht, NL)
CD61 (Y2/51; mM)	MwE(5c)	1:100		DB (Pleasanton, CA, U.S)
CD66b (G10F5; mM)	MwC(5c)	1:150	(D)(E)(F)	BioLegend (San Diego, CA, U.S.)
CD68 (PG-M1; mM)	MwE(3c)	1:200		Agilent
CD123 (9F5; mM)	MwE(3c)	1:50		BD (Franklin Lakes, NJ, U.S.)
CD163 (10D6; mM)	MwE(3c)	1:50		DB

Antibodies (Clone; Source *)	Antigen retrieval (cycles)**	Antibody dilution	Double stain combinations	Source
CD303/BDCA2 (124B3-13; mM)	MwE(5c)	1:100		Dendritics (Lyon, F)
Pan Cytokeratin (MNF116; mM)	MwE(3c)	1:200	(H)	Agilent
CSF-1R (FER216; mM)	MwE(5c)	1:1000		Merck-Millipore (Burlington, MA, U.S.)
CXCR4 (UMB-2; mR)	MwTE(5c)	1:500	(I)	Abcam (Cambridge, GB)
FIBRINOGEN (pR)	None	1:3000		Agilent
GRANZIME-B (11F1; mM)	MwE(3c)	1:20		Leica Biosystem
LAT (LAT-1; mM)	MwE(5c)	1:50	(J)	Agilent
Myeloperoxidase (pR)	None	1:7000	(C)(G)	Agilent
PD-L1 (22C3; mM)	***	1:40		DAKO
PERFORIN (5B10; mM)	MwE(3c)	1:50		Leica Biosystem
TCR AB (8A3; mM)	P	1:50		Thermo Scientific
TCR δ (H-41; mM)	MwE(5c)	1:50		Santa Cruz (Dallas, TX, U.S.)
TIA-1 (TIA-1; mM)	MwE(3c)	1:100		Abcam

* mM: monoclonal Mouse; mR: monoclonal rabbit, pR: polyclonal rabbit

** MwTE(5c): microwave TRIS-EDTA BUFFER pH9.00, 2 cycles at 1000W and 3 cycles at 750W(5 minutes each); MwE(3c): microwave EDTA BUFFER pH 8.00, 3 cycles at 750W(5 minutes each); MwE(5c): microwave EDTA BUFFER pH 8.00, 2 cycles at 1000W and 3 cycles at 750W(5 minutes each); MwC (5c): microwave CITRATE BUFFER pH 6,00, 2 cycles at 1000W and 3 cycles at 750W(5 minutes each); P: Protease 20 minutes at 37°C;

*** PD-L1 staining has been developed on BenchMark Ultra system (Roche), according to the manufacture procedure

RNA in situ hybridization and immunohistochemical analysis

In situ hybridization with V-nCov2019-S-antisense probes specific for the S gene encoding the spike protein (cat.# 845701; accession NC_045512.2; Advanced Cell Diagnostic) was performed using RNAscope 2.5 HD Detection Reagent-BROWN (Advanced Cell Diagnostic) in accordance with the manufacturer's protocol adopting an extended 1 hour incubation in Amp 5 and 30 minutes incubation in Amp 6.

Homo sapiens ubiquitin C (cat.#310041; accession #NM_021009; Advanced Cell Diagnostic) was used as positive control probe.

After evaluation of the ISH result, on the same slide immunostain for CD14 was performed, using antigen unmasking using Target Retrieval Solution pH9 (Novocastra, Leica Biosystems) at 98°C for 15 minutes. The section was brought to room temperature and washed with PBS. After Fc blocking by a specific protein block (BioCare), anti-CD14 (clone EPR3653 Cell Marque, 1:50) primary antibody was applied for 1 hour and staining was revealed using Rabbit on Rodent AP-Polymer (BioCare). Vulcan Fast Red was used as substrate-chromogen, followed by counterstaining with Harris's hematoxylin.

Slides digitalization was performed before and after CD14 stain using an Aperio CS2 digital scanner (Leica Biosystems) with the ImageScope software. Comparison of the single RNA-scope stain and the double stain was performed using the synchronize function.

SARS-CoV2 RNA PCR detection

Viral RNA was extracted from formalin fixed placenta samples. Briefly, the tissue was repeatedly washed for 30 -60 minutes in 1X PBS at room temperature. After the final wash, the tissue was homogenized in 1ml of 1X PBS (10% w/v). Ten microliters of the tissue homogenate were incubated with 1ml of Trizol reagent (Qiagen, Hilden, Germany), and processed according to the manufacturer's instructions. The RNA pellet was resuspended in 50 μ l of H₂O RNase free and used for the Real Time RT-PCR reaction. The SARS-CoV-2 RNA detection was performed using primers and probe targeting gene E, as designed by Corman et al. PCR reactions were performed on 5 μ L of extracted viral RNA in a final volume of 25 μ L, which also contained 12,5 μ l of One Step prime Script III RT-qPCR Mix (Takara, Shiga, Japan) 0.5 μ L of each forward and reverse primer (final concentration 400 nM), 0.5 μ L of probe (final concentration

100 nM). The SARS-CoV-2 RNA was reverse transcribed at 52°C for 15 minutes, followed by 1 cycle of Taq polymerase activation at 95°C for 10 seconds. Amplification consisted of 45 cycles at 95°C for 5 s and 60°C for 30 s. Amplification were performed on a CFX96 Touch Real-Time PCR Detection System (Bio-Rad Laboratories) and data were analyzed with the Software Bio-Rad CFX Manager 3.1.²

Double immunofluorescence for the identification of NETs

For double-marker immunofluorescence, after antigen retrieval, the sections were incubated for 1 hour at room temperature with a combination of the two primary antibodies: histone H3 (Abcam, 1:150) and Myeloperoxidase (Cell Marque, 1:200). The binding of the primary antibodies to their respective antigenic substrates was revealed by made-specific secondary antibodies conjugated with Alexa-488 (Life Technologies, 1:250) and Alexa-568 (Life Technologies, 1:300) fluorochromes. Nuclei were subsequently visualized with DAPI.

Negative staining electron microscopy (nsEM)³

Formalin-fixed tissue fragments (about 0.5 gr each) from respectively the maternal side, the central part and the fetal side of the placenta were rinsed with PBS, then minced with scissors and manually grinded using pestle and mortar with the addition of quartz powder by adding distilled water (10% w/v). The three homogenates were then centrifuged at 10000 rpm for 30 min to eliminate quartz and gross debris and the supernatants finally subjected to negative staining electron microscopy using the Airfuge method (1). Samples were ultracentrifuged (Airfuge, Beckman Coulter Inc. Life Sciences, Indianapolis, Indiana, USA) for 15 min at 82,000xg using a rotor holding six 175- μ l test tubes in which specific adapters for 3mm carbon-coated Formvar copper grids were placed. The grids were then stained using 2% sodium phosphotungstate (pH 6.8) for 1.5min and observed under a Tecnai G2 Spirit Biotwin transmission electron microscope (FEI, Hillsboro, Oregon, USA) at 20,500–43,000x. Attempts to identify the observed viral particles were based on their morphological characteristics.

Transmission Electron Microscopy

For electron microscopy, small tissue fragments formalin fixed were placed in 2.5% glutaraldehyde in cacodylate buffer 0.1 M for 3 hr at 4°C and then post-fixed in 2% osmium tetroxide in the same buffer for 1 hr at 4°C. Dehydration in progressive ethanol concentrations, propylene oxide, and embedding in Epon 812 mixture were performed, as previously described⁴. Semithin (1 μ m-thick) sections cut with an ultramicrotome (Ultracut E- Leica, Microsystems S.r.l., Milan, Italy) using a diamond glass were collected, stained by toluidine blue and examined by light microscopy. For ultrastructural analysis, thin (80 nm-thick) sections obtained from selected zones were collected on 200 meshes-formvar coated copper grids, double stained with uranyl acetate and lead citrate and examined using FEI Tecnai G2 Spirit or CM12 TEM transmission electron microscopes (FEI Instrumentation Company, Hillsboro, Oregon, USA) operating at 85kV. Photographs were taken using a Veleta integrated Digital Camera (Olympus Soft Imaging Solutions, Munster, Germany) and particles size measured by an Olympus Soft Imaging System (iTEM FEI 5.1.30).

Table 2s. Main clinical data of the 15 COVID-19 positive patients and their newborns

Case	1	2	3	4	5	6	7	8	9	10	11	12	13	14	15
Maternal data															
Age (yrs)	29	35	43	44	31	35	39	39	32	42	35	26	39	30	27
Nationality	Italian	Italian	Pakistan	Italian	Italian	Burkina-Fasu	Italian	Italian	Italian	Italian	Italian	Marocco	Italian	Italian	Italian
Obstetric complications (a)	TCP			IUGR PIH				GD	GD						
Gestational age at admission	37+5	38+4	na	33+5	38+6	32+6	39+1	40	40	39+1	39+4	39+1	41+2	40+1	41+3
Comorbidities (a)				OB, ATH	HYT	OB, CHB, HbC		OB				OB			OB
Symptoms (b)	F	F, C, D		F	C, AA	C, D	F, D	C, FM, VD	F, C, AA	F	F				
Lymphocytes (c) x 10 ⁹ /L (0-90-4-00)	0-68	1-87	0-99	1-38	0-75	2-18	1-25	2-01	1-54	2-17	2-27	1-89	2-29	2-92	1-38
PCR (mg/L) < 5-0 (c)	12-8	169	8-4	61	116	93-2	15-8	2-9	34-1	na	na	4-7	2-7	2-4	14-1
AST (U/L) (c) (18-34)	22	71	44	76	30	582	143	not available	21	na	23	41	25	13	na
ALT (U/L)(c) (10-35)	13	42	42	100	29	964	188	13	26	na	9	24	15	9	17
Pneumonia (d)	Yes	Yes	No	Yes	No	Yes	No	No	No	No	No	No	No	No	No
Labor Induction	Yes	No	No	No	No	No	No	Yes	Yes	No	No	No	Yes	No	Yes
Severe maternal morbidity (a)	TCP. PPH	ARDS				ARDS. PPP				PPH					
Neonatal data															
Birth weight (gr)	2-840	2-840	2-850	1-499	3-066	2-159	4-150	3-400	3-190	3-520	2-660	3-850	3-390	3-200	3-210
Stillbirth or neonatal death	No	No	No	No	No	No	No	No	No	No	No	No	No	No	No
APGAR score	9/10	9/10	na	8/9	9/10	1/7	9/9	9/10	9/10	9/10	9/9	9/10	9/10	9/10	9/10
Admission to NICU (days)	Yes (18)	No	No	Yes (18)	Yes (6)	Yes (&)	No	No	No	No	No	No	No	No	No
Severe neonatal morbidity (e)	RDS			HMD. NH. NI. CH	NI	HMD. NEC				PI					
Positive SARS-CoV-2 RT-PCR test	Yes	No	No	No	No	No	No	No	No	No	No	No	No	No	No

na: not available; (&) still hospitalized after ileal resection for NEC

(a): ARDS: acute respiratory disease syndrome. ATH: autoimmune thyroiditis. CHB: chronic HBV hepatitis. GD: gestational diabetes. HbC: congenital Hemoglobinopathy.

HYT: hypothyroidism. OB: obesity. PIH: pregnancy-induced hypertension. PPH: post-partum hemorrhage. PPP: post-partum preeclampsia. TCP: thrombocytopenia.

(b): AA: ageusia/anosmia. C: cough. D: dyspnea. F: fever. FM: fatigue/malaise. VD: vomiting and diarrhea.

(c): worse value during hospitalization (normal range values);

(d): lung chest Xray or lung echography with features of interstitial pneumonia

(e): HMD: hyaline membrane disease. NEC: necrotizing enterocolitis. NI: neonatal infection. PI: perinatal infection. RDS: respiratory disease syndrome.

Table 3s. Main clinical data of the 86 COVID-19 negative patients and their newborns

Maternal data					Newborn data					
CASE	Age (yr)	Morbidities (a)	NP swab for SARS-CoV2 RNA (b)	Gestat. age	Weight (gr) (b)		APGAR (S: stillbirth)		Newborn pathology (c)	
					N1	N2	N1	N2	N1	N2
16	33		ND	38+3	3580		9/9		MP	
17	28	IUGR, PRM	ND	31+4	NA		1/intubated		HMD, J, CMV	
18	41	CA	ND	40+1	3920		9/10		ECS	
19	27	COL, PPH	NEG	36+6	2870	2660	9/10	8/9		RD
20	32		ND	39	2720		9/10			
21	30		ND	36+5	2240	2470	9/10	9/10		
22	38	GH	ND	37+6	3430		9/10			
23	41	PRE	ND	34+6	2400		9/9		HMD, RD	
24	32	HYT	ND	39+2	3730		9/10			
25	37	IUGR	NEG	40	NA		9/10			
26	39		ND	37+4	2360		9/10			
27	28		ND	41+2	2650		4/7			
28	28	PRE, IUGR	ND	35+4	2200		9/9			
29	25		ND	40+3	3078		7/8			
30	34		ND	41+3	3260		9/10			
31	43	VP	ND	36+3	2940		9/10			
32	39		ND	41+2	3548		9/10			
33	41		ND	36+4	2190	2400	9/10	9/10		
34	28	O	ND	37+5	1682		S			
35	31	DG , TPB	ND	27+6	1215		9/9		J, RD	
36	34		ND	39	4540		9/10			
37	41	DM, CHT, PRE, HIV, NP, IUGR,	ND	29	1160		NA			
38	35		NEG	39+4	3060		9/10			
39	39		ND	37+3	2600	2640	9/9	9/9		
40	28		ND	41+3	3660		3/6			
41	30		NEG	39+3	3440		9/10			
42	34	AIAD, HYT, GH	ND	37	2880		9/10			
43	27	OB, GH	NEG	39+2	2900		9/10			
44	33	COL	ND	35+3	2580	2360	9/9	9/9		
45	44	TB	ND	35+5	2730		9/10			
46	25		ND	37+4	2410	2460	9/9	9/10		
47	31		ND	40+6	3570		8/8			
48	34	PRE	ND	35	1878		9/10			
49	38		ND	38+2	3224		9/9			

Maternal data					Newborn data					
C A S E	Age (yr)	Morbidities (a)	NP swab for SARS- CoV2 RNA (b)	Gestat. age	Weight (gr) (b)		APGAR (S: stillbirth)		Newborn pathology (c)	
					N1	N2	N1	N2	N1	N2
50	36		ND	39+5	4630		9/9			
51	27	GH, IUGR	NEG	32+1	997		8/9			
52	44	HYT, TB	ND	34+2	1860		6/8		HMD	
53	29	GD, PF	ND	35+1	NA		NA		PD	
54	23	IUGR	ND	38+3	2306		9/9			
55	25	GD	ND	31+5	1456		NA			
56	37		ND	41	4020		9/9			
57	32	CHT HYT, IUGR	ND	32+4	1700	1880	9/10	7/9		
58	32		ND	41+4	2970		9/10			
59	35		ND	37+4	2300		8/9			HMD
60	22	IUGR	ND	32+1	1484	1657	7/8	8/8		RD
61	38	O, SGA	ND	37+3	1880		9/9			
62	39	DM, CHT, OB, IUGR	ND	34	2082		9/10			
63	36	CMV-s	ND	39	2840		9/10			
64	41	IUGR	ND	33+5	1180		9/9			
65	39	PRE	NEG	31+2	1310		5/8		HMD	
66	34	GD	ND	32+2	1880	1770	8/7	8/9	HMD	HMD
67	34		ND	37+6	2470		10/10			
68	37	EP	ND	36	2710		9/9			
69	41	MPP	ND	36+6	NA		NA			
70	24		ND	37+3	2472	2720	9/10	9/10		
71	30		NEG	37+1	2618	2356	9/10	9/9		
72	24		NEG	39+3	3100		10/10			
73	30	MPP	ND	28+5	840	1000	7/9	6/7		
74	28	GH, IUGR	NEG	36+3	1890		9/9			
75	26	IUGR	NEG	34+4	1690	1650	5/8	5/8	HMD	HMD, J
76	41	IUGR, T21	ND	32+3	NA		S			
77	22		ND	41+2	3320		7/9			
78	30	O, TOX-s	NEG	39	3250		9/9			
79	41		ND	36+2	3400		9/10			
80	38		NEG	39	NA		9/9			
81	37	HYT	NEG	39	3300		9/10			
82	32	O, TTS	NEG	27	1170	750	5/7	2/0		PD
83	29	HYT	NEG	35+3	2860	2960	9/10	8/9		
84	39	PRE	NEG	33+3	1660		9/9		HMD	
85	30	MPP	NEG	29+5	1225		5/9			
86	20	O, FM	NEG	40+5	NA		NA	0		
87	36	MPP	NEG	28+6	998	1130	1/intubated	6/9		
88	30	PRE	NEG	34+2	1600		4/9			

Maternal data					Newborn data					
C A S E	Age (yr)	Morbidities (a)	NP swab for SARS- CoV2 RNA (b)	Gestat. age	Weight (gr) (b)		APGAR (S: stillbirth)		Newborn pathology (c)	
					N1	N2	N1	N2	N1	N2
89	39	NP, CHT, PRE, PKD	NEG	36	2070	2570	9/9	9/9		
90	26	CHT, GD	NEG	37	2500		8/9			
91	21	HYT	NEG	33+6	2520	2480	9/10	7/8		RD
92	40	PREP	NEG	37+1	2610	2350	9/10	9/10		
93	40	HYT, MPP, PRM	NEG	34+4	1340		6/9			
94	35		NEG	38+4	2820		9/10			
95	28	GH	NEG	39	3010		9/10			
96	30	O, TOX-s	NEG	41+1	3160		9/10			
97	34	O, PP	NEG	31+4	1670		9/9			
98	24	CHT, OB, GD	NEG	37+4	2280	2570	7/9	9/9		
99	39		NEG	41+1	3150		9/9			
100	46	O, DC	NEG	32+1	1660	1410	8/9	9/9		
101	32	O, SS, TCP, IUGR	NEG	37	2060		9/10			

a) AIAD: alpha-1-antitrypsin deficiency, CA: chorioamniosis, COL: cholestasis, CHT: chronic hypertension, CMV-s: Cytomegalovirus seroconversion, DC: doppler changes, DM: diabetes mellitus, EP: epilepsy, FM: fetus malformations, GD: gestational diabetes, GH: gestational hypertension, HYT: hypothyroidism, IUGR, intrauterine growth restriction, MPP: major placenta previa, NP: nephropathy, O: others, OB: obesity, PRE preeclampsia, PPH: postpartum hemorrhage, PKD: polycystic kidney disease, PREP: preeclampsia in puerperium, PP: placenta previa, PRM: preterm rupture of membranes, SGA, small for gestational age; SS: Savage syndrome, TB: thrombophilia, T21: trisomy 21, TCP: thrombocytopenia, TPB: preterm birth threatens, TOX-s: Toxoplasma seroconversion, TTS: twin-twin syndrome, VP: vasa previa.

b) ND: not done, NEG: negative, NA: not available

c) ECS: *E. coli* sepsis; HMD: hyaline membrane diseases, J: jaundice, MP: meconium peritonitis, PD: perinatal death, RD: respiratory distress.

1. Table 4s. Main morphological changes observed in the 86 non COVID-19 placentas. Black and grey rectangles indicate the main and minor findings, respectively. MVM: Maternal Vascular Malperfusion. MPFD: Massive Perivillous Fibrin Deposition; FVM: Fetal Vascular Malperfusion; AIP: Acute Inflammatory Pathology; CIP: Chronic Inflammatory Pathology. ^{5,6}

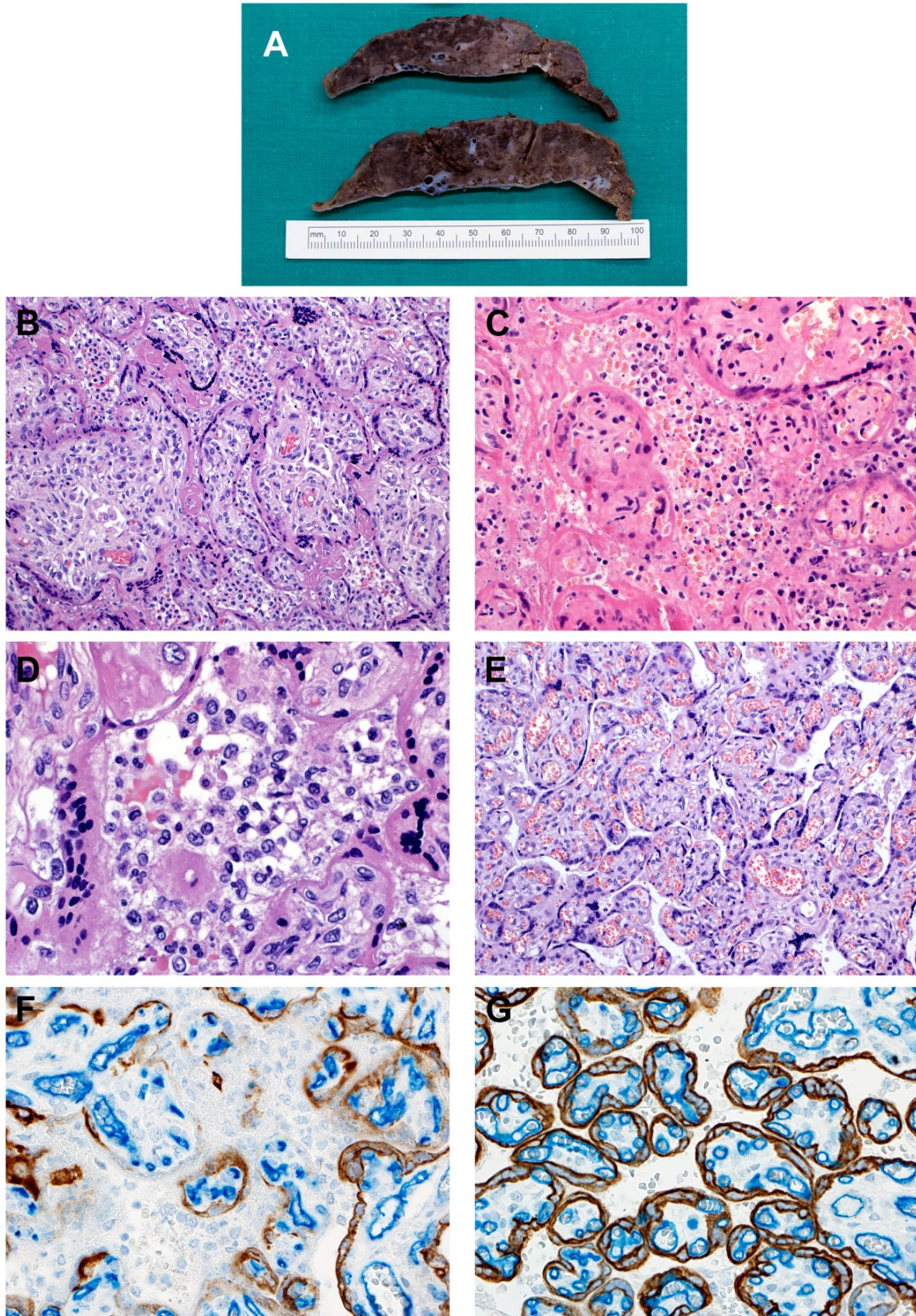
	MVM	Infarcts	Accelerated villous maturation	Decidual arteriopathy	Retroplacental hematoma	Intervillous hematoma	Marginal infarct	Subchorial hematoma	MPFD	FVM	Delayed villous maturation	Chorangiosis	Chorangiomas	Chorionic vessel trombus	AIP	Chorioamnionitis acute	Chorionic vasculitis	Funisitis	CIP	Chronic villitis or chronic villitis and intervillousitis	Deciduitis
16																					
17																					
18																					
19			■													■		■			
20						■															
21							■														
22												■									
23		■																			
24									■												
25												■									
26					■			■													
27																					
28		■		■																	
29																					■
30		■				■											■				
31																					
32																					■
33					■																
34																					
35																					
36			■																		
37													■								
38									■												
39			■										■								
40							■			■											
41			■								■										
42									■									■			■
43																					
44			■									■									
45							■														
46			■						■			■									
47						■										■					

	MVM	Infarcts	Accelerated villous maturation	Decidual arteriopathy	Retroplacental hematoma	Intervillous hematoma	Marginal infarct	Subchorial hematoma	MPFD	FVM	Delayed villous maturation	Chorangiosis	Chorangiomas	Chorionic vessel trombus	AIP	Chorioamnionitis acute	Chorionic vasculitis	Funisitis	CIP	Chronic villitis or chronic villitis and intervillousitis	Deciduitis	
48		■				■			■													
49		■				■	■															
50		■					■															
51		■																				■
52							■		■													■
53																					■	
54																■	■	■				
55																■	■	■				
56																■	■	■				
57			■			■						■										
58		■					■						■									
59			■	■																		
60			■				■															
61						■															■	
62									■			■									■	■
63																					■	
64			■				■															
65		■				■											■					■
66			■																			
67								■	■													
68						■						■										
69											■											
70									■													
71		■										■										
72																	■					
73			■																			
74																	■	■				■
75									■	■							■	■				
76								■	■													
77			■																			
78									■							■	■	■				■
79					■		■		■							■	■	■				
80			■																			
81									■													
82			■						■													
83												■						■				
84						■			■			■										
85									■													
86							■	■	■													
87									■													

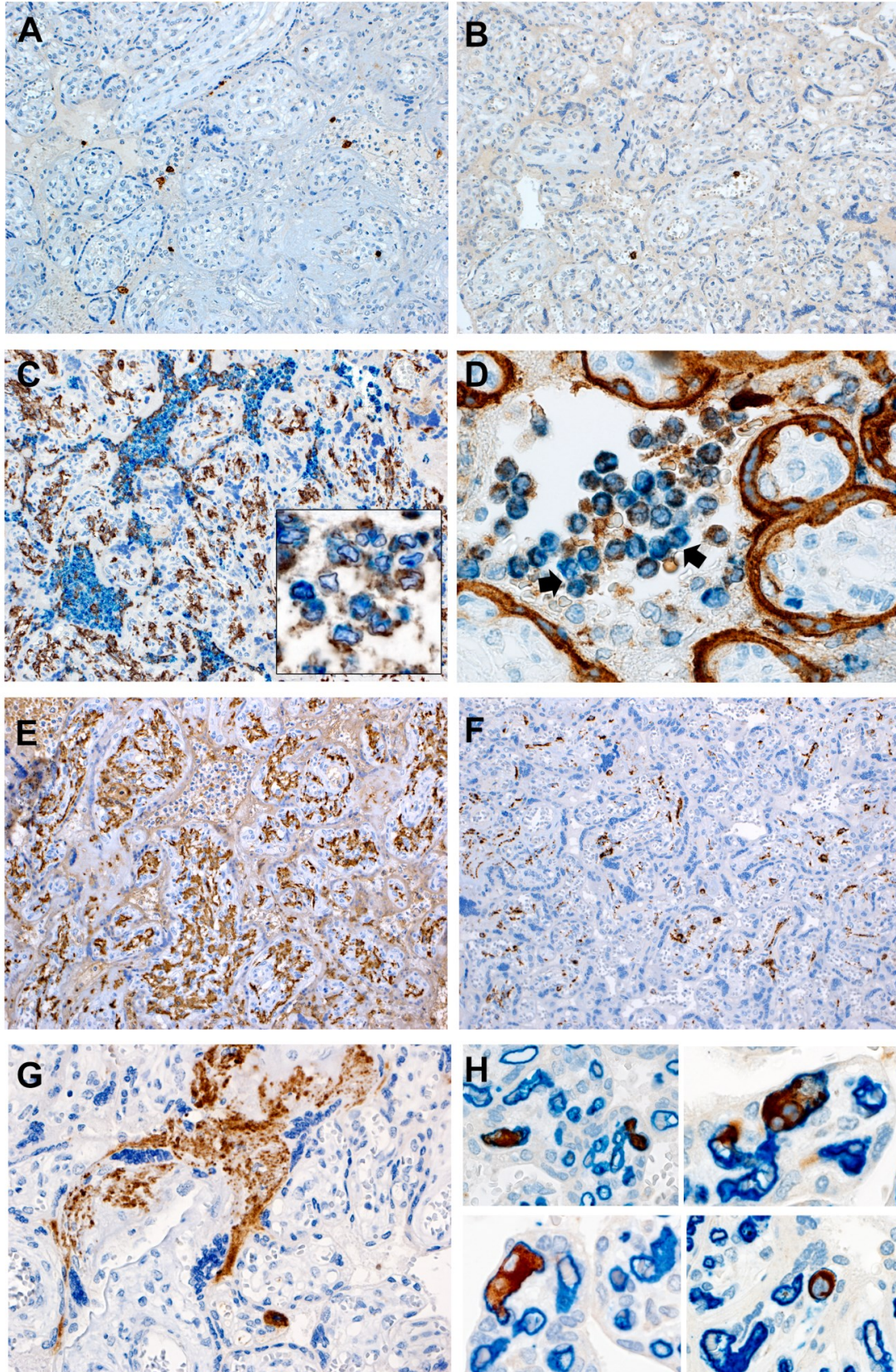
	MVM	Infarcts	Accelerated villous maturation	Decidual arteriopathy	Retroplacental hematoma	Intervillous hematoma	Marginal infarct	Subchorial hematoma	MPFD	FVM	Delayed villous maturation	Chorangiomas	Chorangiomas	Chorionic vessel thrombus	AIP	Chorioamnionitis acute	Chorionic vasculitis	Funisitis	CIP	Chronic villitis or chronic villitis and intervillousitis	Deciduitis	
88		■																				
89									■													
90			■									■										
91								■	■													
92			■						■													
93			■						■													
94			■						■													
95		■						■														
96		■	■						■													
97																■						
98									■			■										
99																					■	
100			■																			
101																■					■	■
Total		11	22	4	3	12	11	5	25		2	13	1	1		17	9	10		7	7	

Supplementary Figure 1. SARS-Cov-2 infected placenta: gross macroscopy, histological and immunohistochemical features of the inflammatory infiltrate and damaged villi.

(A). Cut surface of the placenta: the dark brown chorionic parenchyma contains multiple small whitish areas. (B, C). Intervillous inflammation with marked deposits of fibrin. Villi are relatively preserved in some areas (B), more damaged and necrotic in others (C). (D) Intervillous inflammatory cells are composed of monocyte-macrophages and mature and immature (band) neutrophils. (E) For comparison normal villi in the same placenta in areas uninvolvement by the inflammation (B-C-D-E: haematoxylin and eosin stain). (F, G). Double immunostain for cytokeratin (brown) and CD34 (blue): cytokeratin stain show villi involved by inflammation with thinning or discontinuity of the syncytiotrophoblast cell layer (F), compared with normal villi of the same placenta (G).

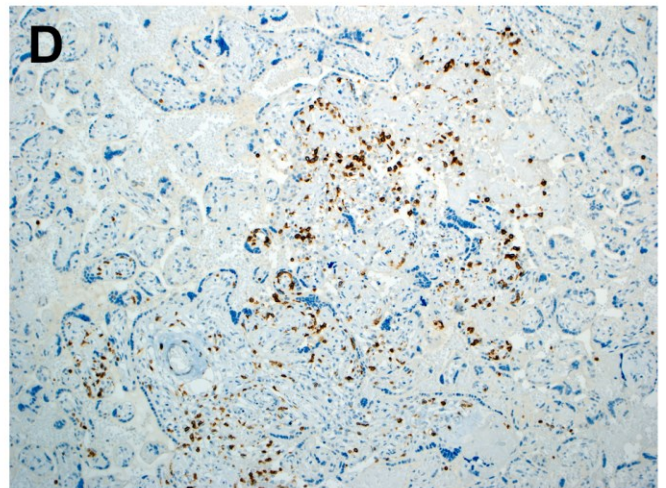
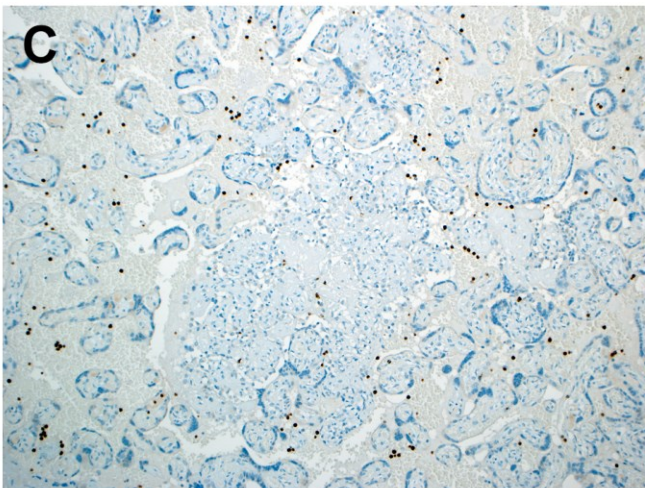
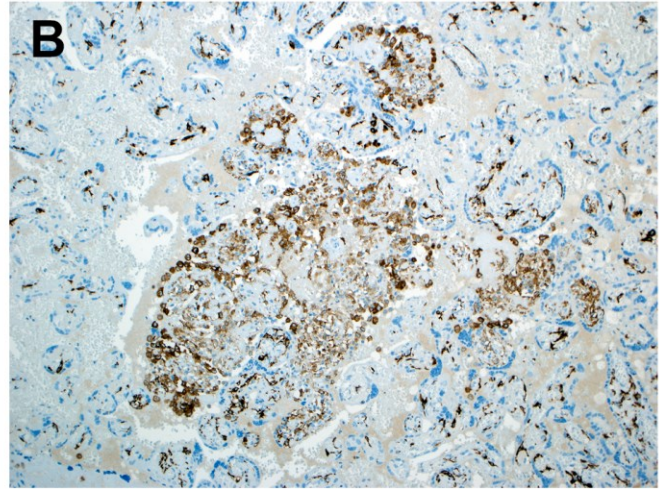
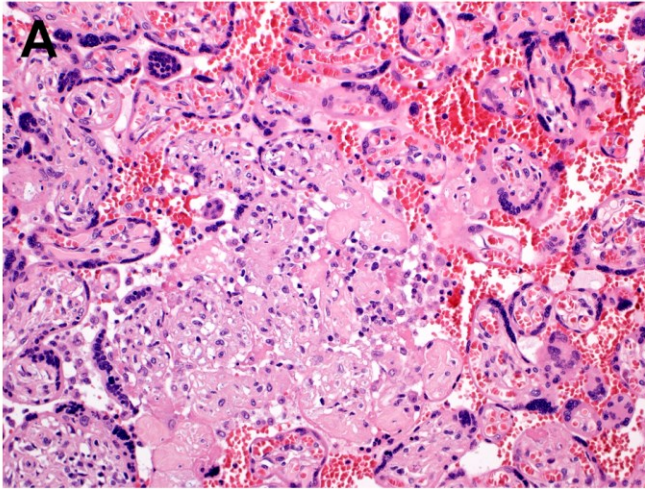


Supplementary Figure 2. Immunostains for the inflammatory cells, Hofbauer cells, platelets and megakariocytes.
 (A, B). Very few lymphoid T-cells (A, immunostain for CD3), B-cells (B, immunostain for CD20) occurred in the placenta. (C and inset) The CD14+ monocyte-macrophages are partially activated and coexpress myeloperoxidase. (double stain for CD14 (blue) and myeloperoxidase (brown)). (D) Neutrophils are composed by immature cells (CD10-, CD66b+, arrows) and mature cells (CD10+, CD66b+). Note positivity of the syncytiotrophoblast for CD10 (Neutral endopeptidase)⁷ (double stain for CD10 (brown) and CD66b (blue)). (E, F). CD163 stain shows the striking difference in the number of Hofbauer cells in Case-1 placenta (E) and in a control (F). (G) Diffuse perivillous deposition of platelets detected by anti-CD61. (H) Examples of intracapillary megakariocytes, whose cytoplasm is stained with anti-CXCR4 (brown); endothelial cells are stained with anti-CD34 (blue).



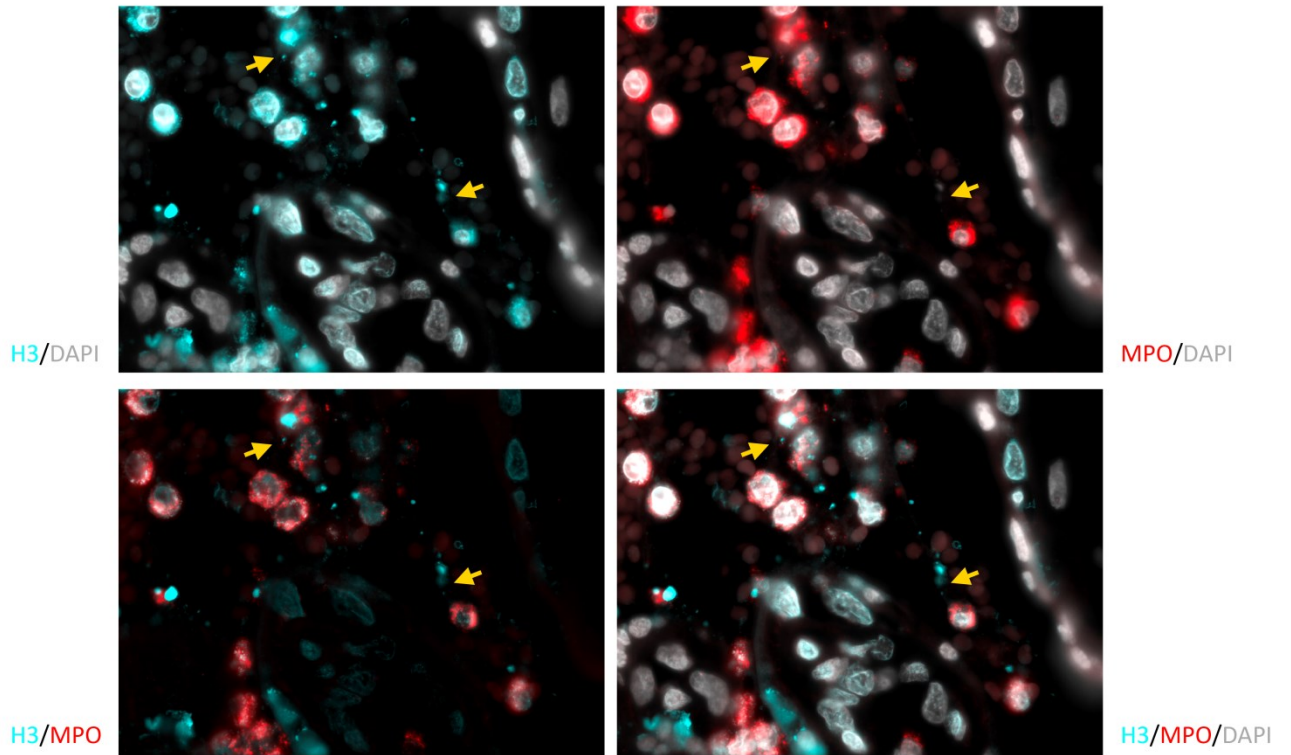
Supplementary Figure 3. A case of placenta from a COVID-19 positive woman (Case#15) showing histiocytic intervillitis and villitis.

Haematoxylin-eosin stain showing a focus of intervillitis (A), that contains numerous CD163 positive monocyte-macrophages (B) and a negligible number of CD66b positive neutrophils (C). CD3+ T lymphocytes are also found in the inflammatory infiltrate as well as in the villus stroma (D).



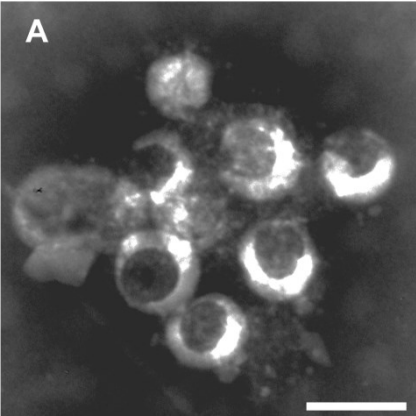
Supplementary Figure 4. Double immunofluorescence for NETs detection

Representative double-marker immunofluorescence microphotographs highlighting the presence of DAPI (white) and H3 cit histone (turquoise) threads associated with MPO-expressing (red) elements, indicative of NET formation (arrows). Original magnification x630



Supplementary Figure 5. Electron microscopy of SARS-2-CoV-2 virus in the infected placenta.

(A) Negative stain electron micrograph of a cluster of viral particles. (Bar 100 nm).



REFERENCES

1. Cigognetti M, Lonardi S, Fisogni S, Balzarini P, Pellegrini V, Tironi A, et al. BAP1 (BRCA1-associated protein 1) is a highly specific marker for differentiating mesothelioma from reactive mesothelial proliferations. *Mod Pathol*. 2015; **28**:1043-57.
2. Corman V, Bleicker D, Brünink S, Drosten C. First case of placental infection with SARS-CoV-2 Diagnostic detection of 2019-nCoV by real-time RT-PCR [Internet]. 2020. Available from: https://www.who.int/docs/default-source/coronaviruse/protocol-v2-1.pdf?sfvrsn=a9ef618c_2 Accessed on June 09, 2020
3. Lavazza A, Pascucci S, Gelmetti D. Rod-shaped virus-like particles in intestinal contents of three avian species. *Vet Rec*. 1990; **126**:581.
4. Capucci L, Scicluna MT, Lavazza A. Diagnosis of viral haemorrhagic disease of rabbits and the European brown hare syndrome. *Rev Sci Tech*. 1991; **10**:347-70.
5. Ernst LM, Sheata BM, McKay E, Chisholm K, Katzman P, Linn R, et al. Diagnostic Pathology Placenta. II ed. Chance D, Geisinger A, Green Terry A, Conno S, Cannon T, Cronin J, editors. Philadelphia, PA: Elsevier; 2015.
6. Khong TY, Mooney EE, Ariel I, Balmus NC, Boyd TK, Brundler MA, et al. Sampling and Definitions of Placental Lesions: Amsterdam Placental Workshop Group Consensus Statement. *Arch Pathol Lab Med*. 2016; **140**:698-713.
7. Fujiwara H, Sato Y, Nishioka Y, Yoshioka S, Kosaka K, Fujii H, et al. New regulatory mechanisms for human extravillous trophoblast invasion. *Reprod Med Biol*. 2005; **4**:189-95.